Supplementary Material for:

Microstructure Defines the Electroconductive and Mechanical Performance of Plant-derived Renewable Carbon Fiber

Qiang Li[1,2,3], Cheng Hu[1,2,3], Heidi Clarke[4], Mengjie Li[1,2,3], Patrick Shamberger[4], Wenhao Wu[5*], Joshua S. Yuan[1,2,3*]

[1]Synthetic and Systems Biology Innovation Hub, Texas A&M University, College Station, TX 77843, USA

[2]Department of Plant Pathology and Microbiology, Texas A&M University, College Station, TX 77843, USA

[3]Institute for Plant Genomics and Biotechnology, Texas A&M University, College Station, TX 77843, USA

[4]Department of Materials Science and Engineering, Texas A&M University, College Station, TX 77843, USA

[5]Department of Physics and Astronomy, Texas A&M University, College Station, TX 77843, USA

*For correspondence: Wenhao Wu: wwu@physics.tamu.edu, Joshua S. Yuan: syuan@tamu.edu

1. Plant cell wall layered structure and manufacturing routes for bioproducts of plant cell wall components

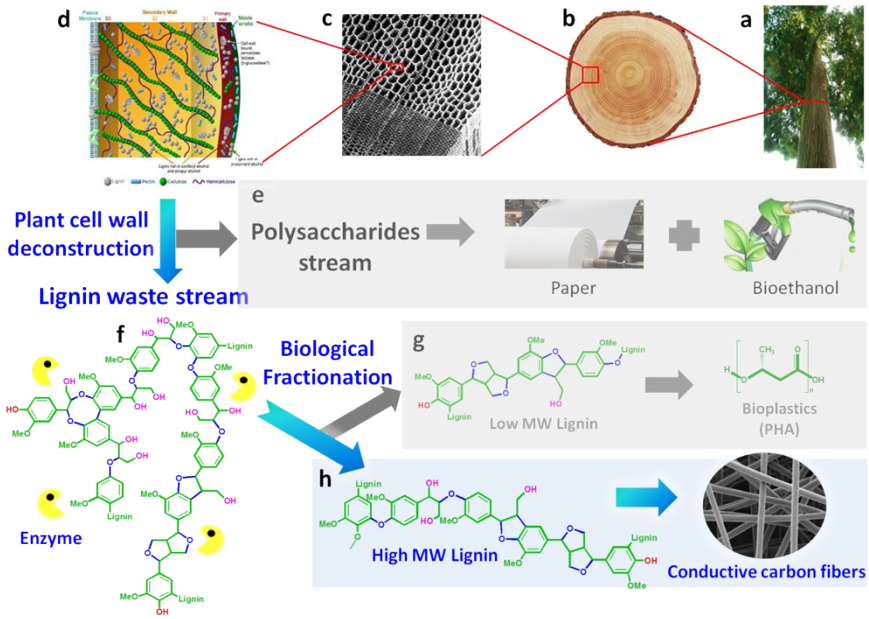

Figure S1. Plant cell wall layered structure and manufacturing routes for bioproducts of plant cell wall components. Images of a tree (a) and wood cross section (b), which displays porous structure (c) made of cell walls. Cell wall components, namely cellulose, hemicellulose, and lignin, are located in different layers of plant cell wall (d). Manufacturing of plant-derived products is initiated by cell wall deconstruction, which refines polysaccharides (cellulose and hemicellulose) and leaves unused lignin as a major waste stream. (e), polysaccharides are manufactured into paper and bioethanol in pulp and paper industry, and lignocellulosic biorefinery industry, respectively. (f), a representative lignin chemical structure, where lignin interunitery linkages, phenolic (Ar-OH) and aliphatic hydroxyl groups (Alk-OH) are in blue, green and pink, respectively. In our research, lignin waste was uniquely fractionated using enzyme to produce a low molecular weight (MW) fraction amenable for bioconversion (g), and a high molecular weight fraction suitable for conductive carbon fiber (h). Images in (c) and (d) were adapted from Uraki et al (2011)[1] and Achyuthan et al (2010),[2] respectively.

2. Experimental

2.1 Materials

Alkali Kraft lignin (370959) from softwood used in this research was purchased from Sigma–Aldrich, USA. Polyacrylonitrile (PAN) with molecular weight of 150,000 g/mol was purchased from Pfaltz & Bauer, USA. *N,N*-dimethylformamide (DMF, 99.8%) and other chemicals used were products of Sigma–Aldrich, USA.

2.2 Lignin enzymatic treatment

The enzymatic treatment of Kraft lignin was performed as we reported previously.[1] Briefly, Kraft lignin was treated with laccase (15 mg/g lignin), 1-hydroxy benzotriazolehydrate (HBT, 25 mg/g lignin) and oxygen supply (flow rate 5 ccm) at a 10 wt% concentration for 48 h in a Biostat® A reactor (Sartorius, Bohemia, NY). The temperature and the stirring speed were controlled at 50 ^{o}C and 200 rpm, respectively. The water-soluble and water-insoluble lignin fractions can be obtained by centrifuging the samples after the enzymatic treatment. The former fraction was then precipitated out against pH 2 de-ionized water, and followed by washing three times with 200 mL of pH 2 de-ionized water. The water-insoluble fraction was also washed three times as the water-soluble fraction. Both water-soluble and water-insoluble lignin fractions were then lyophilized to get dry lignin powder.

2.3 Lignin characterizations

2.3.1 ^{31}P nuclear magnetic resonance spectroscopy (^{31}P NMR)

To reveal the reaction mechanism of lignin under laccase-mediator, the hydroxyl groups in lignin were extensively analyzed by using ^{31}P NMR.[3-5] Briefly, about 40 mg of lignin was firstly

dissolved in a pyridine/$CDCl_3$ solution (400 μL, 1.6:1, V/V). After complete dissolution, relaxation reagent (chromium(III) acetylactonate, 50 μL, 11.4 mg/mL in pyridine/$CDCl_3$) and internal standard (cyclohexanol, 100 μL, 10.85 mg/mL in pyridine/$CDCl_3$) were added into lignin solution, which was followed by the addition of the phosphitylation reagent (2-chloro-4,4,5,5-tetramethyl-1,3,2-dioxaphospholane, TMDP, 100 μL). Before transferring the mixture into a NMR tube (5 mm O.D.), the phosphitylation reaction was further kept for 30 min at room temperature. ^{31}P NMR spectra were acquired under a Varian NMRS-500RM by using a 90° pulse with 25-s pulse delay and 256 acquisitions.[4-5]

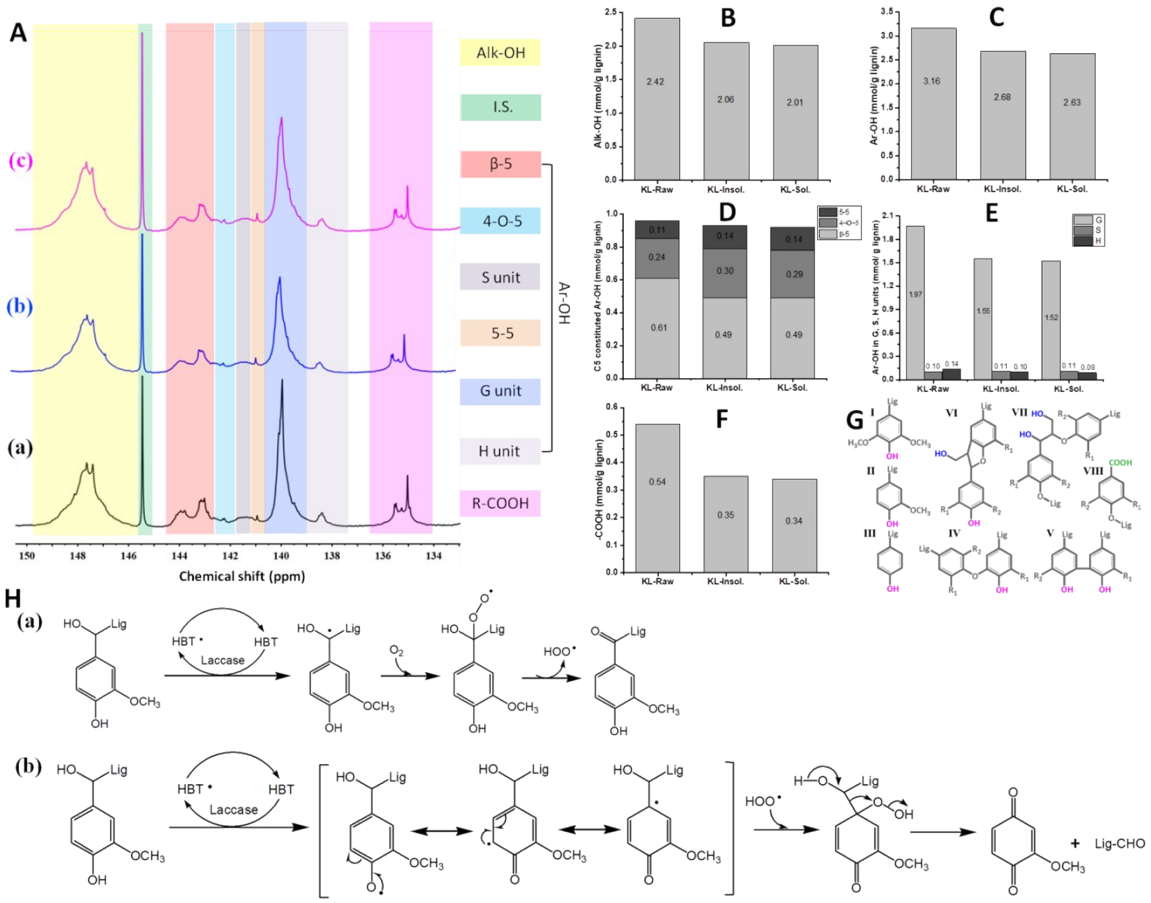

Figure S2. The content of hydroxyl groups in lignin measured by ^{31}P NMR. A, ^{31}P NMR spectra of KL Raw (a), KL-Insol. (b), and KL-Sol. (c); B, the content of aliphatic hydroxyl groups (Alk-

OH); C, the content of phenolic hydroxyl groups (Ar-OH); D, Ar-OH in C5 substituted lignin units (IV, V, and VI in G); E, Ar-OH in syringyl (S), guaiacyl (G), and *ρ*-hydroxyphenyl (H) units; F, the content of carboxylic acid (-COOH) in lignin; G, hydroxyl groups (Ar-OH in magenta, Alk-OH in blue) in representative lignin units of syringyl (I), guaiacyl (II), *ρ*-hydroxyphenyl (III), 4-O-5 (IV), 5-5 (V), *β*-5 (VI), and *β*-O-4 (VII). Carboxylic acid (green) is shown in VIII in panel G. 4-O-5, 5-5, and *β*-5 represent C5 substituted lignin units; H, possible reaction mechanism of lignin under laccase-mediator treatment, which lignin could undergo benzylic hydrogen abstraction (a) and phenolic hydrogen abstraction (b). I.S. is internal standard, and Lig in panel H represented lignin moiety.

2.3.2 Two-dimension heteronuclear single quantum coherence NMR spectroscopy (2D HSQC NMR)

Analysis of lignin using 2D HSQC NMR and the semi-quantification were as we reported previously.[6] Briefly, 150 mg of acetylated lignin were analyzed using a Bruker AVANCE 500 MHz spectrometer. The integration and semi-quantification of both lignin units and linkages were carried out using the software MestReNova. The aromatic regions of HSQC spectra were shown in Figure S3. The dominated guaiacyl (G) peaks and trace syringyl (S) peaks were detected. The volume integration of the peaks of G_2 and $S_{2/6}$ at δC/δH 113.3/7.0 ppm and δC/δH 103.8/6.7 ppm, respectively, were measured. The S integrals were logically halved. For all raw and fractionated lignin, the G units were at about 92 %. This result is consistent with the ^{31}P NMR characterization that G units dominated the Kraft lignin we used, which further indicated that this lignin is a softwood lignin.

In our previous paper,[6] we have reported the linkage profiles of the relative frequencies, which were calculated from the ratio of the volume integration of each linkage to that of all linkages. Here we calculated the linkage profiles based on 100 aromatic groups (%), which were the volume integrations of G (G_2, δC/δH 113.3/7.0 ppm) and S ($S_{2/6}$, δC/δH 103.8/6.7 ppm) units. The results were as shown in Figure S4. The raw Kraft lignin had 8.35 *β-O*-4 linkages per 100 aromatic groups (8.35 %), and water-soluble lignin had lower *β-O*-4 (7.72%), while water-insoluble lignin had higher *β-O*-4 (8.77%). Even though these data were much lower than before we calculated as the relative content (61.5%, 57.1% and 68.5% for raw lignin, water-soluble lignin and water-insoluble lignin, respectively), the changes of the data were in consistence.

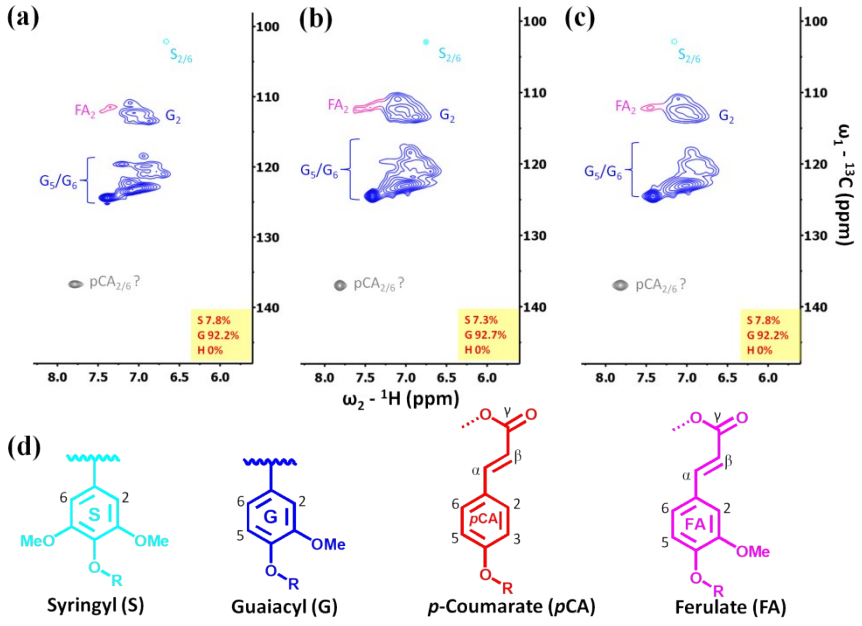

Figure S3. Aromatic regions of 2D HSQC NMR spectra of lignin samples. Panel a, b and c are KL-Raw, KL-Sol., and KL-Insol., respectively. The chemical structures of S, G, *p*CA and FA are in panel d. The chemical shifts of these structures are in Table S1.

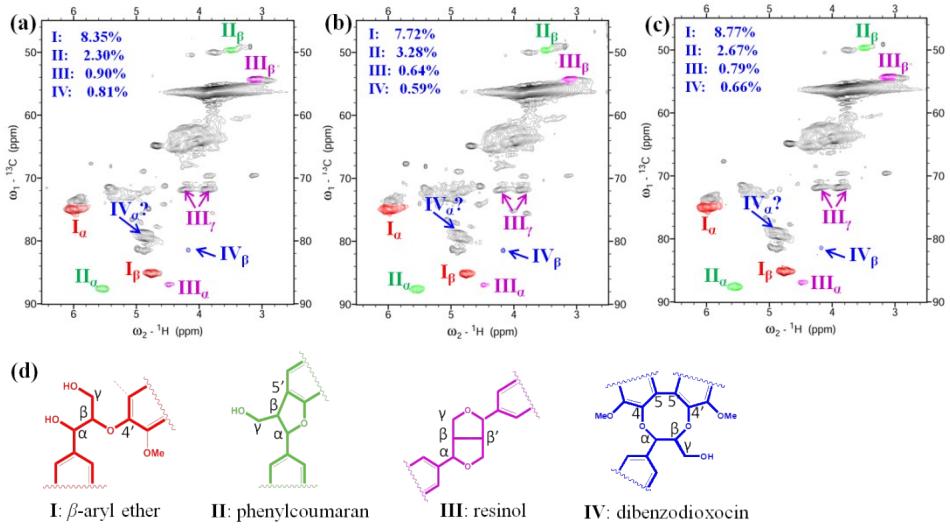

101

102 Figure S4. Aliphatic regions of 2D HSQC NMR spectra of lignin samples. Panel a, b and c are
103 KL-Raw, KL-Sol. and KL-Insol., respectively. The chemical structures of different lignin
104 linkages are in panel d. The chemical shifts of these linkages are in Table S1. The frequencies as
105 shown in each panel were calculated based on 100 aromatic groups (%).

106 Table S1. Assignments of lignin chemical structures in 2D HSQC NMR.[1, 2]

Lignin structures and units*		F2 (ppm)	F1 (ppm)
Aliphatic region	Iα (α position in β–*O*–4')	6.0	74.5
	IIα (α position in β–5')	5.5	87.7
	IIIα (α position in β–β')	4.5	87.0
	IVβ (β position in DBDO)	4.2	81.5
Aromatic region	C_2/H_2 in guaiacyl units (G_2)	7.0	111.3
	$C_{2,6}/H_{2,6}$ in ρ-hydroxyphenyl units ($H_{2/6}$)	n.d.	n.d.
	$C_{2,6}/H_{2,6}$ in syringyl units ($S_{2/6}$)	6.7	103.8
	$C_{2,6}/H_{2,6}$ in *p*-Coumarate ($pCA_{2,6}$)	7.6	130.0
	C_2/H_2 in Ferulate (FA_2)	7.5	111.5

107 *Units and linkages are shown in Figure S3d and Figure S4d, respectively. n.d., not detected.

2.3.3 Viscosity

The viscosity of wet spinning dopes (lignin/PAN blend and pure PAN) at the range of 600 s^{-1} to 0.1 s^{-1} was measured as before.[6] As shown in Figure S5, all lignin/PAN dopes had much lower viscosity than pure PAN, which could be accounted for the much higher molecular weight of the PAN polymer (150,000 g/mol) than lignin. For fractionated lignin samples, the water-insoluble lignin/PAN dope had higher viscosity than that of raw lignin/PAN dope, while the water-soluble lignin/PAN dope had decreased viscosity. These results were in consistent with the changes in lignin molecular weight, which water-insoluble lignin fraction (22965 g/mol) had increased molecular weight as compared with the raw lignin (8592 g/mol) but the water-soluble lignin (3197 g/mol) had decreased molecular weight.[6] The changes in lignin molecular weight could thereof render the changes of the viscosity of lignin/PAN dopes.

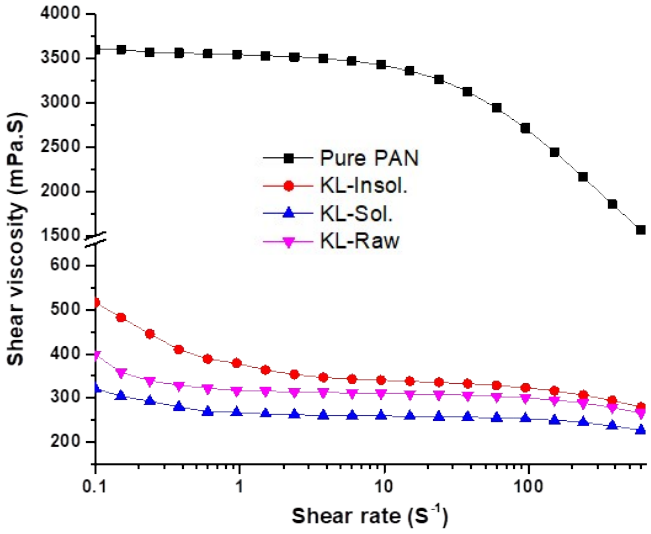

Figure S5. Viscosity of lignin/PAN dopes in DMF.

2.4 Carbon fiber preparation

2.4.1 Wet spinning

A homemade wet spinning unit was used to spin lignin into fibers. Lignin and PAN were firstly ground to pass a 60-mesh screen, and then mixed each other at a weight ratio of 50%:50%. The lignin/PAN mixture was dissolved in DMF at 60 ^{o}C with the concentration of 10 % to prepare the spinning dopes. The as-prepared dopes were then sonicated by using a Branson 1510 sonicator for 2-h before spinning to remove existed air bubbles. In the spinning process, the dopes were injected into a methanol/DMF coagulation bath (-20 ^{o}C) using a micro-pump with the resolution of 0.73 μL/h (NE-300, New Era Pump Systems Inc., Farmingdale, NY) to form fibers. The injection rate for all spinning was 0.08 mL/min. As-spun fibers were winded onto a rolling drum. After washing with deionized water, the fibers were cut and hanged under 15 g load until dry.

2.4.2 Thermostabilization

As-spun lignin precursor fibers were thermostabilized under atmosphere using a muffle furnace (GSL 1200X, MTI Corporation, Richmond, CA). The as-spun fibers were placed in crucibles. Heating was from room temperature to 250 ^{o}C at a rate of 1 ^{o}C/min, which was followed by holding the samples at 250 ^{o}C for 1 h before the furnace was automatically cooled down.

2.4.3 Carbonization

To prepare carbon fibers, as-thermostablized fibers were then carbonized in a split tube furnace with vacuum system (GSL 1600X, MTI Corporation, Richmond, CA) under argon gas

flow (240 cm^3/min). The temperature for carbonization was increased from room temperature to 1 000 ^oC with a heating rate of 5 ^oC/min and then held at 1000 ^oC for 1 h before the furnace was automatically cooled down.

2.5 Carbon fiber characterizations

2.5.1 Field emission scanning electron microscope (FE-SEM)

The morphologies of carbon fibers and fiber cross sections were observed under a Quanta 600F FE-SEM (FEI Company, Hillsboro, OR) with 5kV accelerating voltage and 10 mm working distance. Prior the observation, carbon fibers were coated with 10 nm iridium (Ir). In order to get the morphologies of cross sections, fibers were mounted vertically on the SEM sample holder. For each carbon fiber, more than 40 different fibers were measured to get an average diameter.

As shown in Figure S6, lignin-based precursor fibers were prepared by a wet-spinning set-up. The average diameters of the resultant carbon fibers after carbonization at 1000 ^oC were at micron-scale level (33 to 36 μm, Figure S6C4-F4). The analysis of morphology and diameter showed that the enzymatic fractionation has significantly improved macro structures of the resultant carbon fibers. As shown in Figure S6C3-F3, carbon fiber made of un-fractionated lignin had defects of pores and debris on the cross section, yet the carbon fibers made from both water-insoluble and water-soluble lignin fractions displayed flat-layer-like transverse textures, which was similar to that of the pure PAN carbon fiber. For diameter distribution, the percentage of carbon fibers within the most frequent 3 μm diameter range were 86.4% within 33-36 μm for carbon fibers made from

water-insoluble lignin/PAN (Figure S6D4) and 85.0% within 36-39 μm for carbon fibers made from water-soluble lignin/PAN (Figure S6E4). Both percentages were much higher than that made from un-fractionated lignin/PAN (57.5% within 33-36 μm, Figure S6C4). All of these improvements in carbon fiber macrostructures correlated to the enhancement in microstructures and in the functionality for both mechanical and electroconductive performances.

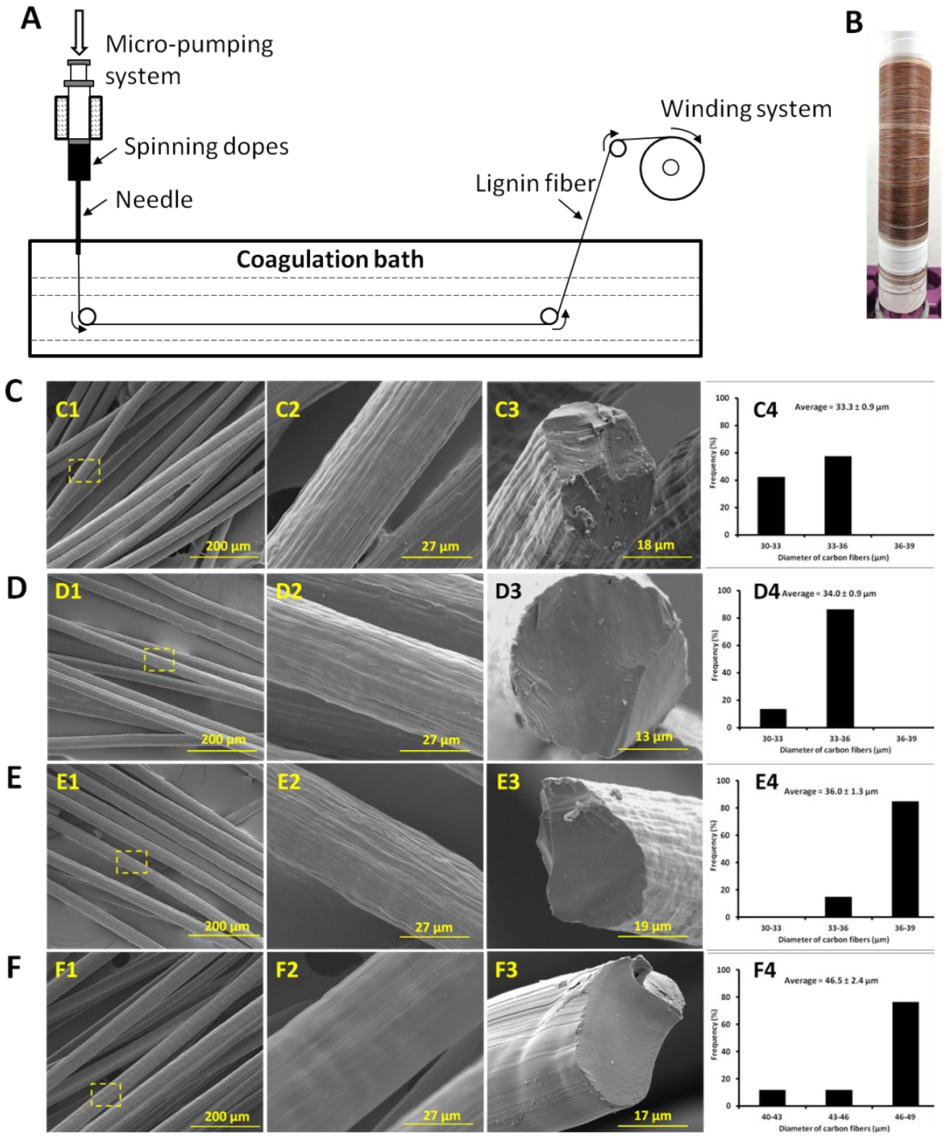

Figure S6. The wet-spinning set-up for making lignin fibers (A) and the as-spun fibers collected on the wind drum (B). SEM of carbon fibers were in C to F. C, D, E, and F were carbon fibers made of KL-Raw, KL-Sol, KL-Insol., and pure PAN, respectively. The histograms in C4 to F4 showed the diameter distributions of the corresponded carbon fibers. KL-Raw, raw Kraft lignin; KL-Insol., the insoluble fraction from laccase-mediator treated Kraft lignin; KL-Sol., the soluble fraction from laccase-mediator treated Kraft lignin.

2.5.2 Mechanical test

The mechanical strength of carbon fibers was measured by using a TestResources universal mechanical tester (Shakopee, MN). Carbon fibers were mounted on a paper sample holder with the help of super glue. The sample holder was then fixed on two grippers for the measurement. The force applied to samples was controlled by using with a 2 N load cell that has a resolution of 0.0001 N. The displacement was controlled by an actuator with a position resolution of 0.06 mm. The displacement rate was set at 0.200 mm/min for all tests. The applied force (F) and the corresponding displacement (d) were synchronously monitored during the measurement. The original length (L) of fibers was measured by using a vernier caliper. To get the area (A) of each fiber, the morphologies of the cross sections of carbon fibers were observed under aforementioned FE-SEM after the test. The area was then calculated using the software ImageJ®. Stress-strain curves were plotted after getting stress (σ) and strain (ε) using the equations of $\sigma = F/A$ and $\varepsilon = d/L$, respectively. The tensile strength represented the maximum stress at fracture and the modulus of elasticity (MOE) was obtained from the slop of the elastic deformation region in a stress-strain curve. Elongation (%) was calculated by $d'/L \times 100$, where d' is the displacement at the fracture. For each sample, at least 15 fibers were measured to give an average result.

2.5.3 Electric conductivity measurement

The conductivity of the carbon fibers was measured by using a Fluke 87 TRUE RMS multimeter. The measurement was as shown in Figure S7. A single fiber was fixed by silver paint (GC Electronics) onto a cover glass, and then the electrical resistance (R, Ω) of the fibers between two silver paints was measured with the multimeter at ambient atmosphere. The electrical conductivity (σ, S/m) was calculated from the equation of $\sigma = 1/\rho = L/(R \times A)$, where ρ is electrical resistivity (Ω.m), L (m) and A (m^2) are the length and the cross section area of the fiber as measured, respectively. The length (L) of the fiber was measured by using the aforementioned vernier caliper. To calculate the area (A) of fiber cross section, the diameter of each fiber was measured under a Zeiss Axiophot microscope after the conductivity test, and at least 25 points on one fiber were measured to give an average fiber diameter.

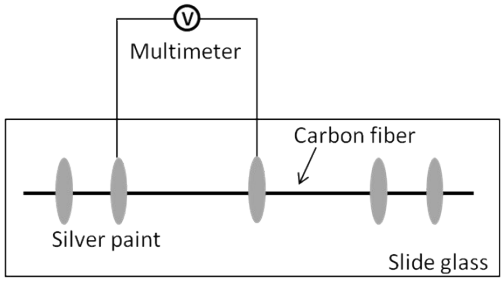

Figure S7. Schematic set-up of electrical conductivity.

2.5.4 X-ray diffraction (XRD)

XRD analysis of carbon fiber crystallite structures was performed under a Bruker D8 Discovery XRD (Bruker, Madison, WI). To avoid the orientation preference, carbon fibers were ground into fine powders by an agate mortar and pestle before the measurement. X-ray resource was generated at 40 kV voltage and 40 mA current with Cu Ka wavelength (λ) of 1.542 Å. Scanning range (2θ) was from 8^o to 55^o, scanning step size was 0.05^o, and scanning rate was set

at 1.5°/min. The crystalline size (L_{hkl}) was calculated from (002) panel around 2θ 24.5° in the XRD diffractograms using Scherrer equation: $L = \frac{K\lambda}{\beta \cos\theta}$, where L is the crystalline size, nm; K is shape factor, set as 0.94 in this calculation; λ is the X-ray wavelength (1.542 Å); β is the full width at half maximum (FWHM) in radian; θ is the Bragg angle in degree. The distance between two crystalline lattices (d_{hkl}) was estimated by using Bragg's law: $2d\sin\theta = n\lambda$, where d is distance in nm; θ is the Bragg angle in degree; n is set as 1. As shown in Figure S8, the d_{hkl} between each lignin fractions after the enzyme-mediator fractionation was similar to that of raw Kraft lignin, indicated that the distance between two crystalline lattices in lignin-based carbon fibers was not significantly improved. In comparison with lignin-based carbon fiber, pure PAN-based carbon fiber had smaller d_{hkl} (0.356 nm), which could be attributed to the high molecular weight and the uniform molecule structure of PAN polymers.[4, 6]

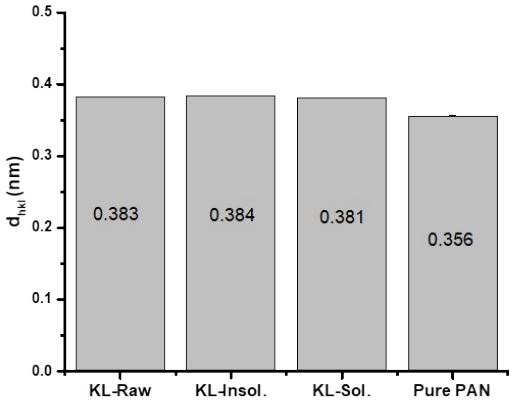

Figure S8. The distance between two crystalline lattices (d_{hkl}) in carbon fibers as calculated from Bragg's law.

2.5.5 Raman spectroscopy

The ground carbon fiber powder was mounted on a glass slide with the help of a double adhesive tape, and Raman spectra were taken under a Horiba Jobin-Yvon LabRam Raman

Confocal Microscope with 633 nm laser, 10× magnification of objective lens, D0.3 filter, 200 μm confocal pinhole, 10 s exposure time, and 10 accumulations. The D band (1348 cm^{-1}) and G band (1581 cm^{-1}) in Raman spectra were deconvoluted by Guassian curve fitting method using Origin 9 software. The G/D ratios were calculated from the area ratios of these two bands.

3. Reference

1. Uraki, Y. et al. Fabrication of honeycomb-patterned cellulose material that mimics wood cell wall formation processes. *Mater. Sci. Eng. C* **31**, 1201-1208 (2011).

2. Achyuthan, K.E. et al. Supramolecular self-assembled chaos: Polyphenolic lignin's barrier to cost-effective lignocellulosic biofuels. Molecules 15, 8641 (2010).

3. Crestini, C., Argyropoulos, D.S. Structural analysis of wheat straw lignin by quantitative ^{31}P and 2D NMR spectroscopy. The occurrence of ester bonds and α-O-4 substructures. *J. Agr. Food Chem.* **45**, 1212-1219 (1997).

4. Li, Q. et al. Tuning hydroxyl groups for quality carbon fiber of lignin. *Carbon* **139**, 500-511 (2018).

5. Pu, Y., Cao, S. & Ragauskas, A.J. Application of quantitative ^{31}P NMR in biomass lignin and biofuel precursors characterization. *Energy Environ. Sci.* **4**, 3154-3166 (2011).

6. Li, Q. et al. Quality carbon fibers from fractionated lignin. *Green Chem.* ***19***, 1628-1634 (2017).